# Molecular dynamics study of the effect of grain size on the melting point of nanocrystalline aluminum

© *G.M. Poletaev*[1], *A.A. Sitnikov*[1], *V.Yu. Filimonov*[1,2], *V.I. Yakovlev*[1], *V.V. Kovalenko*[3]

[1] Polzunov Altai State Technical University,
Barnaul, Russia
[2] Institute for Water and Environmental Problems SB RAS,
Barnaul, Russia
[3] Siberian State Industrial University,
Novokuznetsk, Russia

E-mail: gmpoletaev@mail.ru

Using molecular dynamics simulation, the influence of the average grain size and excess energy due to the presence of grain boundaries on the melting point of nanocrystalline aluminum was studied. In the considered range of grain sizes from 2.5 to 10 nm, the difference between the melting point and the melting point of a pure crystal turned out to be inversely proportional to the average grain size and directly proportional to the excess energy. Melting proceeded heterogeneously and began primarily from grain boundaries. When studying recrystallization in nanocrystalline aluminum, it was found that it occurs more intensely as the temperature approaches the melting point, as well as at a smaller initial grain size.

## 1. Introduction

Much attention has been paid in recent years to ultra-fine grained and especially nanocrystalline materials, which include polycrystals with an average grain size of less than 100 nm. They have unusual physical and mechanical properties associated mainly with a large volume fraction of grain boundaries compared to the usual coarse-grained state [1–4]. They are obtained by various methods, including intensive plastic deformation, sintering of nanopowders, physical vapor deposition, etc. A high degree of non-equilibrium of the structure and large values of excess or stored energy is a common property of nanocrystalline materials [1–4].

The experimentally observed decrease of the ignition temperature of the high-temperature synthesis reaction in the production of intermetallides after preliminary mechanical activation treatment of the initial powder mixture apparently should be considered as one example of the manifestation of excess energy in nanocrystalline materials [5–10]. The original mixture is subjected to intense mechanical stress as a result of such treatment frequently resulting in the formation of nanocrystalline structure with a high concentration of structural defects in metals [8–10]. The ignition temperature coincides equals to the aluminum melting point under the normal conditions, but it significantly decreases after mechanical activation treatment [5–10]. Relatively high values of excess energy due to the high concentration of grain boundaries and other defects in the mixture after mechanical activation, high diffusion mobility of atoms in

nanocrystalline materials, as well as a possible decrease of the melting point of nanocrystalline aluminum compared with conventional coarse-grained aluminum are referred as the main reasons for such decrease.

As for the decrease of the melting point of nanocrystalline aluminum, it was shown using computer modeling in [11–15] that melting is not a homogeneous process, it begins, as a rule, with free surfaces and grain boundaries. In addition, the melting of the structure near the interface began in the above studies at lower temperatures than in case of a single crystal. The nanocrystalline structure has a relatively high proportion of non-equilibrium grain boundaries, which, obviously, should affect the overall melting process and the phase transition onset temperature. Studying phase transitions in nanoparticles [16–18] we actually observed a noticeable decrease of the melting point of metal particles with a nanocrystalline structure.

This paper is devoted to the study of the impact of the average grain size on the melting point of nanocrystalline aluminum using molecular dynamic modeling. Generally, maintaining the constant average grain size, especially in cases of small values of the order of several nanometers [12,14,15], during the entire simulation of nanocrystal heating is one of the main problems in solving this issue. The smaller the grain size, the more intensive is the recrystallization and growth of the average grain size at high temperatures. We used a special technique in this paper to maintain permanent average size which will be described in detail below. The study also addressed the

impact of excess energy on the melting point. Besides the impact of temperature and grain size on the intensity of recrystallization was studied.

## 2. Model description

The interatomic interactions in the molecular dynamics model was described using the EAM potential from Ref. [19] where it was obtained based on comparison with experimental data and *ab initio* calculations of various properties of aluminum. This potential reproduces quite well a wide range of mechanical and structural-energy properties [19–21], it has proven itself well in various molecular dynamics studies and has been successfully tested in modeling of various processes, including melting, crystallization and self-diffusion in melt [19–22].

The calculation cell had the shape of a parallelepiped and contained from 80,000 to 340000 atoms, depending on the grain size. The nanocrystalline structure was created as follows. The centers of future grains were determined in the initially ideal FCC crystal of aluminum depending on the given average grain size $d$. These centers were located in the volume of the calculation cell similarly to the nodes of the HCP lattice (not atoms, but grain centers) with a distance between the nearest nodes, grain centers, equal to $d$. The structure around each center in spheres with a diameter of 0.8 of the grain size (the closest distance between the centers) was rotated in space at random angles. The structure inside the spheres was fixed and the rest of the structure was subjected to melting followed by modeling of crystallization at a temperature of 700 K for 500 ps. The structure was cooled to 0 K at the final stage.

The structure in the grain centers in spheres with a diameter of 0.3 of the average grain size remained fixed throughout the modeling to prevent any impact on the results of recrystallization and grain growth during the modeling, especially for small grains. All computer experiments for comparison were also performed without fixing the structure in the grain centers. Melting, as will be shown below, began from the grain boundaries, and the fixation of the structure in areas of a given size (0.3 of diameter) had practically no effect on the value of the temperature of the onset of melting.

Grains with the size range from 2.5 to 10 nm were considered. It was difficult to determine the melting point of nanocrystalline aluminum for grains of smaller size. As the grain size increased, its impact on the melting point decreased. The sections of calculated cells with grains of 4 and 8 nm are shown in Figure 1 using the crystal phase visualizer based on the CNA (Common Neighbor Analysis) method [23]. Blue atoms are atoms with the immediate environment corresponding to the FCC crystal structure, white atoms are atoms with unidentified crystal lattice or with an amorphous structure, gray atoms are atoms that were stationary during the modeling. The grains had the
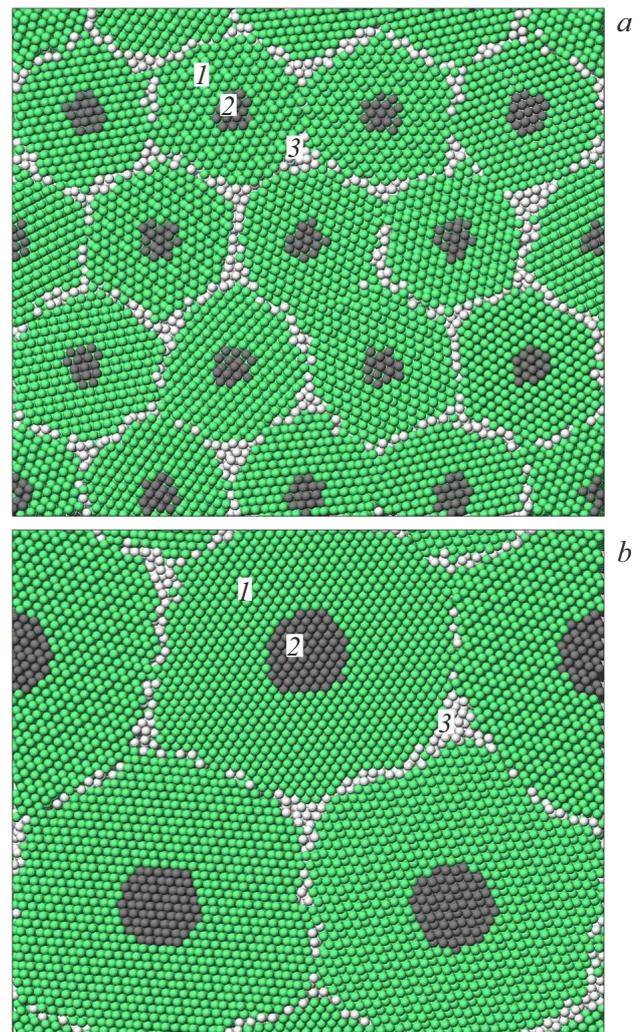


**Figure 1.** Cross sections of calculation cells of nanocrystalline aluminum with an average grain size: *a*) 4 nm; *b*) 8 nm. *1* — atoms with immediate environment corresponding to the FCC crystal lattice; *2* —the atoms that remained stationary during the simulation; *3* — the crystal lattice was not identified.

shape of regular hexagons in cross section as can be seen from Figure 1.

Periodic boundary conditions and an NPT canonical ensemble with a Nose−Hoover thermostat were used in the model. The pressure was kept constant and equal to zero during modeling, and therefore the calculation cell could freely change the volume during heating and melting. The thermal expansion in case of temperature variations was taken into account, including thermal expansion in the fixed areas in the grain center. The time integration step was 2 fs.

The gradual heating method was used for determining the melting point with the plotting of the dependence of the average potential energy of atoms on the temperature, which is often used in similar tasks [12,16–18,24]. The heating was performed at a rate of $10^{12}$ K/s. It is obvious, that the lower the heating rate, the more accurate is the determination of

the temperature of the onset of phase transition. But, on the other hand, the longer the computer experiment is, the higher is the impact of recrystallization and transformation of the grain structure on the obtained results. The rate of $10^{12}$ K/s turned out to be optimal in this case.

## 3. Results and discussion

Figure 2 shows the dependences of the average atomic energy on the temperature for nanocrystalline aluminum with an average grain size of 4 nm (Figure 2, *a*) and 8 nm (Figure 2, *b*) in case of heating at a constant rate of $10^{12}$ K/s with the fixation of the structure in the central regions of the grains (curves *2*) and without fixation (curves *3*). Curves (indicated by a number *1*) obtained by heating of an ideal crystal that does not contain any defects and a free surface are provided for comparison. In the latter case, the melting point turned out to be significantly higher (1180 K) than the found melting points of nanocrystalline structure. Melting began already at a temperature of 780 K with an average grain size of 4 nm, it started at a temperature of 920 K with an average grain size of 8 nm. The melting process was homogeneous in the case of single-crystal aluminum, which does not contain any defects and a free surface, i.e. it was almost simultaneous in the entire volume of the calculation cell and for this reason the increase of the energy of atoms at the moment of melting (curves *1*) is more sharp on Figure 2 compared to the curves *2* and *3*.

The melting began at the grain boundaries if the calculation cell contained any grain boundaries and then the liquid crystal interphase boundary moved from the boundaries into the rest of the volume. That is, melting in this case had a heterogeneous mechanism, when the crystal-liquid front moves at a finite speed, which depends on temperature and, as a rule, equals to several tens of meters per second [25,26]. We did not observe the presence of a fixed crystal-liquid front that after formation usually moved until the melting of the entire calculation cell. For this reason we determined the melting point based on the moment of the onset of the phase transition (shown by the arrows in Figure 2), which, in turn, was determined by the intersection of the approximation lines before and after the onset of melting.

Four main differences can be distinguished when comparing the dependencies obtained for the average grain size 4 nm (Figure 2, *a*) and 8 nm (Figure 2, *b*). Firstly, the melting of nanocrystalline aluminum with a smaller average grain size begins at a lower temperature (approximately 780 K for 4 nm grains and 920 K for 8 nm grains). That is, the average grain size does influence the melting point. Secondly, the recrystallization of grains with the size of 4 nm was much more intensive, which is evident from the difference in dependencies *2* and *3* in this case. The formation of the melting front and the corresponding increase of the potential energy of the atoms without fixation of the grain centers (curve *3*) was followed by the drop of
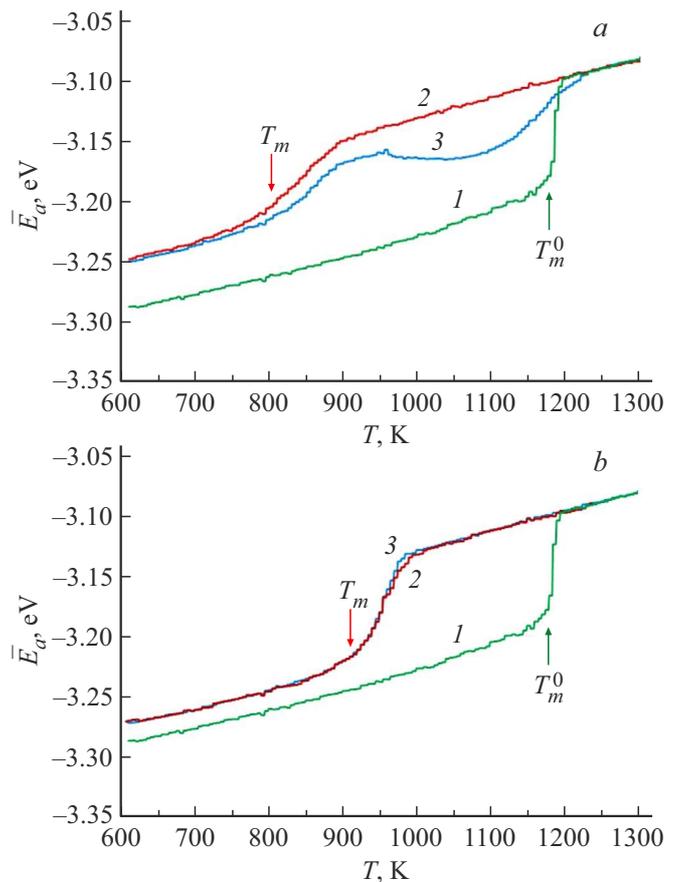


**Figure 2.** Dependences of the average potential energy of atoms on temperature in case of heating at a rate of $10^{12}$ K/s for an ideal crystal (curves *1*) and nanocrystalline aluminum (curve *2* — without fixation of the structure in the grain centers, curve *3* — with fixation) with an average grain size of 4 nm (*a*) and 8 nm (*b*).

energy due to the recrystallization process. The curves *2* and *3* almost coincided with an average grain size of 8 nm which indicates a weak contribution of recrystallization in this case. Thirdly, the growth of the potential energy of atoms during the movement of the melting front is slower with a smaller grain size. The fourth difference lies in the greater difference of the initial values of the average energy of atoms in nanocrystalline and single-crystal structures with an average size of 4 nm, which is obviously explained by the higher density of the boundaries in the case of smaller grain sizes.

Figure 3, *a* shows the dependence of the melting point of nanocrystalline aluminum on the average grain size. The values obtained in case of fixation of the structure in the grain centers are shown with colored markers while blank markers show the values obtained without fixation of the structure. In the second case, the melting point was determined by the first bend of the dependence of the average energy of atoms on temperature (for example, as in the case of the curve *3* in Figure 2, *a*), regardless of the further drop of the energy because of the recrystallization.
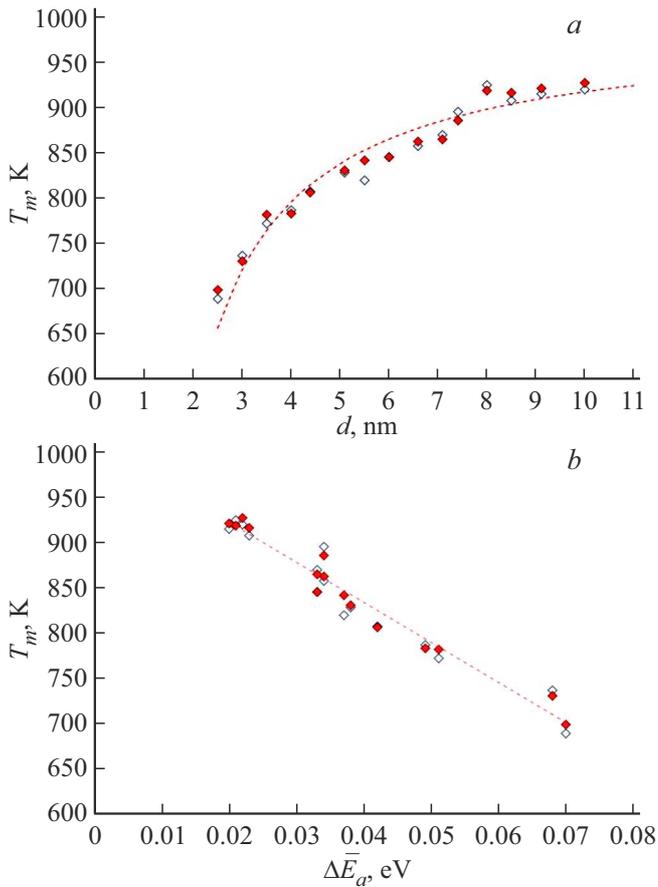
**Figure 3.** Dependencies of the melting point of nanocrystalline aluminum on: *a*) the average grain size; *b*) the amount of excess energy per atom. Markers — the model results, dotted lines — the approximation.

Melting begins from the grain boundaries owing to the relatively easier destruction of the crystal structure near them because the atoms in the defects are located in shallower quantum wells compared to an ideal crystal and it is easier for them to leave the quantum wells in the result of thermal vibrations. Atoms near the crystal-liquid front on the side of the crystalline phase are also located in relatively shallower quantum wells than in the crystal volume because of the more disordered arrangement of atoms from the side of the melt. In addition, self-diffusion is more intensive in the melt and the free volume is bigger compared to the free volume in the crystal, which is also the reason for easier crystal destruction near the crystal-liquid front than inside the crystal volume, and the reason for the movement of the front.

The mechanism of decrease of the melting point of nanocrystalline materials is close to the mechanism of decrease of the melting point of nanoparticles, where melting begins from the surface and spreads deep into the particles. A simple formula is often used for a mathematical description of the effect of the free surface of nanoparticles on their melting point. This formula is based on the assump-tion that the change of the phase transition temperature compared to a massive sample is proportional to the ratio of the surface area of the particle to its volume [27–33]. I. e., this change should be inversely proportional to the particle diameter in case of a round particle. We used the same assumption for describing the dependence of the melting temperature of the nanocrystalline structure on the average grain size, adding a correction $\delta$ that takes into account the final thickness of the grain boundaries

$$T_m(d) = T_m^0\left(1 - \frac{\alpha}{d - \delta}\right). \tag{1}$$

Here $T_m$ and $T_m^0$ — the melting temperatures of the nanocrystalline structure and single crystal; $\alpha$ — the parameter responsible for the degree of impact of grain boundaries on the melting point.

The dotted line in Figure 3, *a* shows the approximation curve found using the formula (1). As can be seen the values obtained in the model (round markers in the figure) match the approximation curve quite well, which confirms the leading role of grain boundaries in the process of melting of a nanocrystalline structure. Values of the quantities for the formula (1): $T_m^0 = 990$ K, $\alpha = 0.71$ nm, $\delta = 0.4$ nm. It should be noted that $T_m^0$ coincided with the value of the melting point of an aluminum crystal in the presence of a free surface, which we found in [22] using the same potential. The value $\delta$, which has a sense of the average width of grain boundaries, turned out to be close to the width determined when measuring grain boundary diffusion (0.5−0.6 nm) [34.35]. The dependence found is close to the obtained dependences of the melting temperature of round nanoparticles on their diameter [27–33]. Moreover, the value calculated for the nanocrystalline structure $\alpha$ (0.71 nm) falls within the range of values given in different sources for aluminum nanoparticles in vacuum: $\alpha$ ranges from 0.6 to 1.2 nm depending on the approach and inter-atomic potential [31–33].

We constructed the dependence of the melting temper-ature on the excess energy per atom, $\Delta \bar{E}_a$ in addition to the dependence on the average grain size $d$ (Figure 3, *b*). The excess energy was defined as the difference between the average values of the potential energy of an atom in the subject structure before modeling of heating and in an ideal crystal: $\Delta \bar{E}_a = \bar{E}_a - \bar{E}_a^0$. The obtained dependence turned out to be close to a linear dependence within the considered range of values of $\Delta \bar{E}_a$ with the approximation line equation $T_m = -4425\Delta \bar{E}_a + 1010$ (shown by dotted line).

The data obtained in the model are listed in the table. The values of the average number of atoms in grains $\bar{N}_g$ and the ratio of the grain boundary area to the volume of the calculation cell $S/V$ are provided in the table in addition to the above mentioned values. In the latter case, as can be seen, the values of $S/V$ linearly correlate with the excess energy $\Delta \bar{E}_a$ suggesting that the excess energy in this model is determined mainly by the proportion of grain boundaries in the cell volume.

Sections of a calculation cell with a nanocrystalline structure with an average grain size of 8.5 nm at different melting points are shown in Figure 4 using a crystal phase visualizer. The fixation of the structure in the grain centers
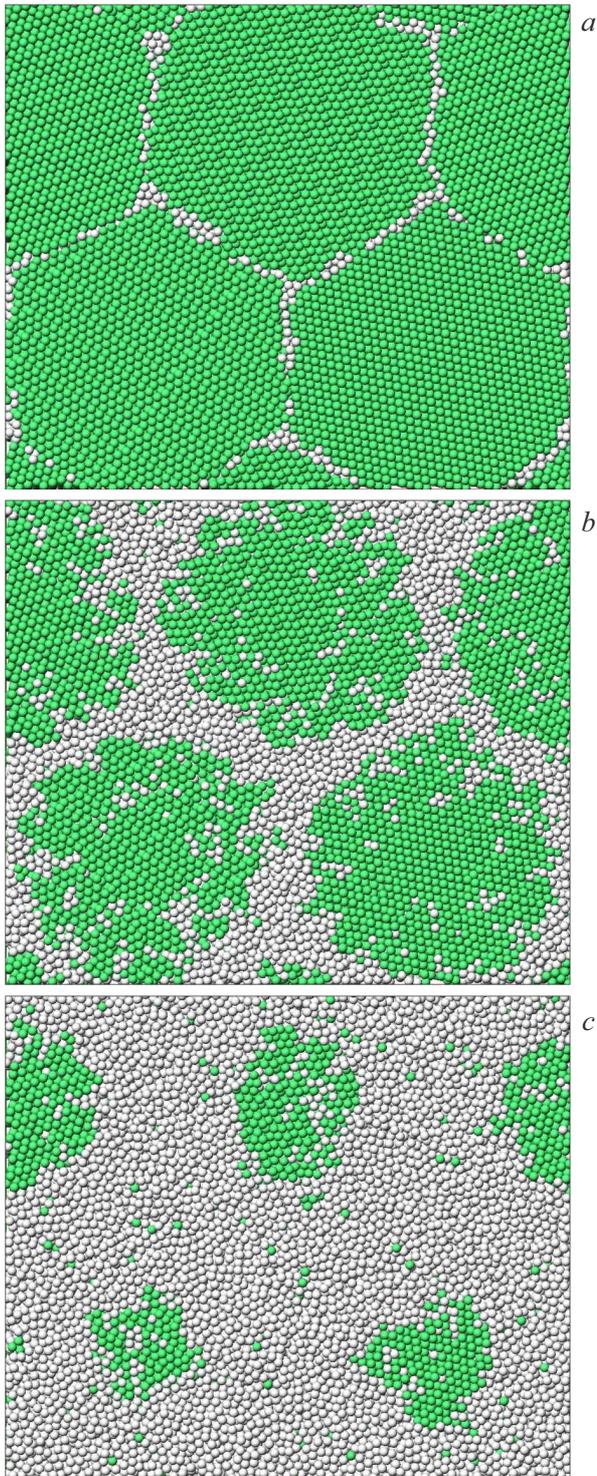


**Figure 4.** Melting from grain boundaries in a calculation cell with an average grain size of 8.5 nm during heating at a rate of $10^{12}$ K/s: *a*) initial structure; *b*) structure at a temperature of 950 K; *c*) structure at a temperature of 985 K.
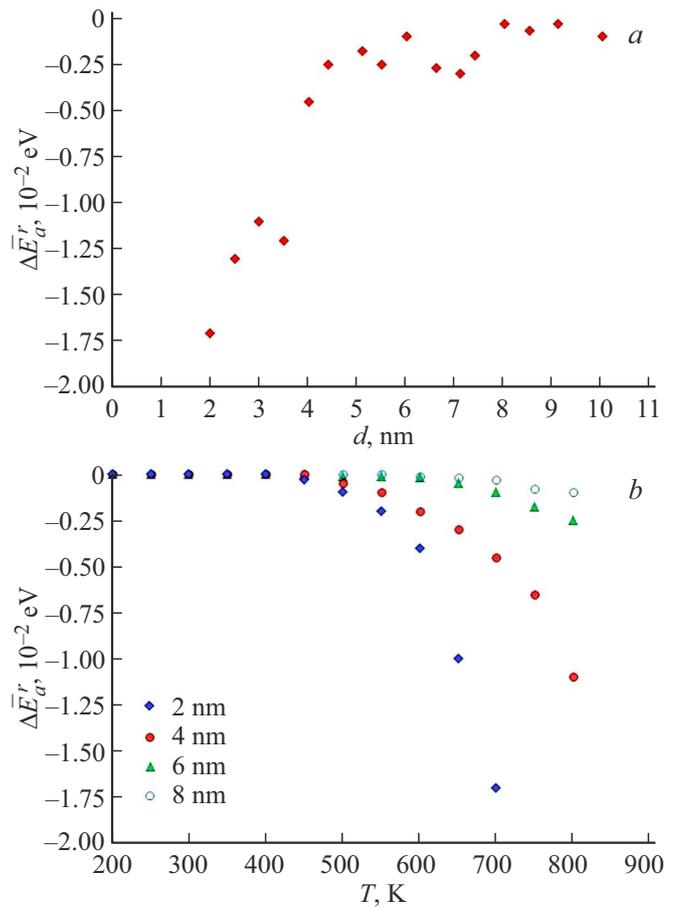
**Figure 5.** Dependences of the change of the average potential energy of an atom during relaxation process at a constant temperature for 300 ps: *a*) on the average grain size at a temperature of 700 K; *b*) on the temperature for four values of the average grain size: 2, 4, 6 and 8 nm.

was not used in this case. The figure clearly shows that melting begins at the grain boundaries, that is, where the atoms are located in shallower quantum wells compared to an ideal crystal. Then the crystal-liquid front moves from the boundaries to the center of the grains, which melts in the last turn as seen in Figure 4, *c*.

It should be noted that not all grain boundaries equally acted as melting initiation sites. It depends on the energy of the boundary formation, that is, again, on the excess energy. The melting from boundaries with low energy of formation, for example, small-angle, special boundaries with a high density of coincident nodes and especially twins, began at higher temperatures than melting in the case of large-angle boundaries.

An intensive recrystallization was observed during modeling of heating, as mentioned above, especially in the case of small grain sizes. The concentration of defects decreased and grains grew during recrystallization. We conducted an additional study of the impact of grain size and temperature on the amount of decrease of the average potential energy

The average number of atoms in a grain $\bar{N}_g$, the ratio of the grain boundary area to the volume of the calculation cell $S/V$, excess energy $\Delta \bar{E}_a$, melting temperatures without fixation $T_m^0$ and with fixation $T_m^f$ of the structures in the grain centers depending on the average grain size $d$

| $d$, nm | $\bar{N}_g$ | $S/V$, nm$^{-1}$ | $\bar{E}_a$, eV | $T_m^0$, K | $T_m^f$, K |
|---|---|---|---|---|---|
| 2.5 | 702 | 0.788 | 0.070 | 689 | 699 |
| 3 | 1103 | 0.764 | 0.068 | 737 | 730 |
| 3.5 | 1824 | 0.592 | 0.051 | 772 | 782 |
| 4 | 2744 | 0.550 | 0.049 | 786 | 783 |
| 4.4 | 3450 | 0.491 | 0.042 | 807 | 806 |
| 5.1 | 5616 | 0.433 | 0.038 | 828 | 830 |
| 5.5 | 6979 | 0.411 | 0.037 | 820 | 842 |
| 6 | 9261 | 0.370 | 0.033 | 845 | 845 |
| 6.6 | 12167 | 0.369 | 0.034 | 857 | 862 |
| 7.1 | 15625 | 0.342 | 0.033 | 870 | 865 |
| 7.4 | 17576 | 0.319 | 0.034 | 895 | 885 |
| 8 | 21952 | 0.269 | 0.021 | 924 | 918 |
| 8.5 | 26108 | 0.262 | 0.023 | 907 | 916 |
| 9.1 | 32768 | 0.239 | 0.020 | 915 | 921 |
| 10 | 42875 | 0.221 | 0.022 | 920 | 927 |
| single-crystal | − | 0 | 0 | 990 | 990 |

of an atom during relaxation. The fixation of the structure in the grain centers was not used. Figure 5, $a$ shows the dependence of the change of the average energy of an atom on the grain size during relaxation at a constant temperature of 700 K for 300 ps. The change of the average potential energy of an atom was calculated as the difference between the average energies at the beginning of the computer experiment and after 300 ps: $\bar{E}_a^r = \bar{E}_a(t_0) - \bar{E}_a(t)$. As can be seen, recrystallization was more intensive as the grain size decreased and the change of the average energy of atoms was higher in this case. Recrystallization had the highest intensity in the case of grain sizes below 4 nm.

The dependences of the change of the average potential energy of atoms on the temperature during relaxation for 300 ps are shown in Figure 5, $b$. Constant temperature was maintained during these experiments. Dependences were obtained for four values of the average grain size: 2, 4, 6, and 8 nm. The recrystallization was more intensive with an increase of the temperature, especially when the temperature approached the melting point. The dependences are close to exponential, which is probably attributable to the determining roles of self-diffusion and migration of grain boundaries in the recrystallization process, the intensities of which are known to have an exponential (Arrhenius) dependence on the temperature. The transformation of the structure was more intensive during relaxation at the same temperature, as already shown using the dependence in Figure 5, $a$.

## 4. Conclusion

The impact of the average grain size and excess energy on the melting point of nanocrystalline aluminum was studied using molecular dynamic modeling. It is shown that the smaller the average grain size is and the greater the excess energy is due to the presence of grain boundaries the lower is the melting point. In addition, the difference between the melting temperature in the considered grain size range from 2.5 to 10 nm and the melting temperature of a single crystal is inversely proportional to the average grain size and decreases linearly with an increase of the excess energy.

The melting was more heterogeneous in the modeled polycrystal and began primarily from the grain boundaries, after which the melting front moved towards the rest of the volume. Melting in the model was homogeneous in an ideal crystal that does not contain any defects and any free surface, that is, melting was immediate throughout the entire volume, and began at a temperature significantly higher than in the case of presence of grain boundaries (by more than 250 K compared, for example, with a nanocrystal with an average grain size 10 nm).

It was found in the result of study of the recrystallization in nanocrystalline aluminum that it proceeds more intensively when the temperature approaches the melting point, as well as with a smaller initial grain size, that is, with a higher density of grain boundaries.

## Conflict of interest

The authors declare that they have no conflict of interest.

# References

[1] H. Gleiter. Acta Mater. **48**, *1*, 1 (2000).
https://doi.org/10.1016/S1359-6454(99)00285-2

[2] M.A. Meyers, A. Mishra, D.J. Benson. Prog. Mater. Sci. **51**, 427 (2006). https://doi.org/10.1016/j.pmatsci.2005.08.003

[3] K.S. Kumar, H. Van Swygenhoven, S. Suresh. Acta Mater. **51**, 5743 (2003). https://doi.org/10.1016/j.actamat.2003.08.032

[4] T.D. Thangadurai, N. Manjubaashini, S. Thomas, H.J. Maria. Nanostructured Materials. Springer (2020). 221 p.

[5] N.F. Shkodich, A.S. Rogachev, S.G. Vadchenko, N.V. Sachkova, R. Chassagnon. Int. J. Self-Propag. High-Temp. Synth. **21**, 104 (2012).
https://doi.org/10.3103/S1061386212020100

[6] F. Maglia, C. Milanese, U. Anselmi-Tamburini, S. Doppiu, G. Cocco, Z.A. Munir. J. Alloys Compd. **385**, 269 (2004). https://doi.org/10.1016/j.jallcom.2004.03.142

[7] F. Maglia, C. Milanese, U. Anselmi-Tamburini. J. Mater. Res. **17**, *8*, 1992 (2002). https://doi.org/10.1557/JMR.2002.0295

[8] A.S. Rogachev, N.F. Shkodich, S.G. Vadchenko, F. Baras, D.Yu. Kovalev, S. Rouvimov, A.A. Nepapushev, A.S. Mukasyan. J. Alloys Compd. **577**, 600 (2013).
http://dx.doi.org/10.1016/j.jallcom.2013.06.114

[9] V.Y. Filimonov, M.V. Loginova, S.G. Ivanov, A.A. Sitnikov, V.I. Yakovlev, A.V. Sobachkin, A.Z. Negodyaev, A.Y. Myasnikov. Combust. Sci. Technol. **192**, *3*, 457 (2020). https://doi.org/10.1080/00102202.2019.1571053

[10] M.V. Loginova, V.I. Yakovlev, V.Yu. Filimonov, A.A. Sitnikov, A.V. Sobachkin, S.G. Ivanov, A.V. Gradoboev. Lett. Mater. **8**, *2*, 129 (2018).
https://doi.org/10.22226/2410-3535-2018-2-129-134

[11] S.R. Phillpot, J.F. Lutsko, D. Wolf, S. Yip. Phys. Rev. B **40**, 2831 (1989). https://doi.org/10.1103/PhysRevB.40.2831

[12] S. Xiao, W. Hu, J. Yang. J. Phys. Chem. B **109**, *43*, 20339 (2005). https://doi.org/10.1021/jp054551t

[13] S. Xiao, W. Hu, J. Yang. J. Chem. Phys. **125**, *18*, 184504 (2006). https://doi.org/10.1063/1.2371112

[14] T. Wejrzanowski, M. Lewandowska, K. Sikorski, K.J. Kurzydlowski. J. Appl. Phys. **116**, *16*, 164302 (2014). https://doi.org/10.1063/1.4899240 15.

[15] Z. Noori, M. Panjepour, M. Ahmadian. J. Mater. Res. **30**, 1648 (2015). https://doi.org/10.1557/jmr.2015.109

[16] G.M. Poletaev, Y.V. Bebikhov, A.S. Semenov. Mater. Chem. Phys. **309**, 128358 (2023).
https://doi.org/10.1016/j.matchemphys.2023.128358

[17] G. Poletaev, Y. Gafner, S. Gafner, Y. Bebikhov, A. Semenov. Metals **13**, *10*, 1664 (2023).
https://doi.org/10.3390/met13101664

[18] G.M. Poletaev, Y.Y. Gafner, S.L. Gafner. Lett. Mater. **13**, *4*, 298 (2023). https://doi.org/10.22226/2410-3535-2023-4-298-303

[19] R.R. Zope, Y. Mishin. Phys. Rev. B **68**, 024102 (2003). https://doi.org/10.1103/PhysRevB.68.024102

[20] Y.-K. Kim, H.-K. Kim, W.-S. Jung, B.-J. Lee. Comput. Mater. Sci. **119**, 1 (2016).
https://doi.org/10.1016/j.commatsci.2016.03.038

[21] Q.-X. Pei, M.H. Jhon, S.S. Quek, Z. Wu. Comput. Mater. Sci. **188**, 110239 (2021).
https://doi.org/10.1016/j.commatsci.2020.110239

[22] G.M. Poletayev, R.Yu. Rakitin. FTT **64**, *4*, 412 (2022). (in Russian). https://doi.org/10.21883/FTT.2022.04.52180.247

[23] H. Tsuzuki, P.S. Branicio, J.P. Rino. Comput. Phys. Commun. **177**, 518 (2007). https://doi.org/10.1016/j.cpc.2007.05.018

[24] T.D. Nguyen, C.C. Nguyen, V.H. Tran. RSC Advances **7**, 25406 (2017). https://doi.org/10.1039/C6RA27841H

[25] W.-L. Chan, R.S. Averback, D.G. Cahill, Y. Ashkenazy. Phys. Rev. Lett. **102**, 095701 (2009).
https://doi.org/10.1103/PhysRevLett.102.095701

[26] H.Y. Zhang, F. Liu, Y. Yang, D.Y. Sun. Sci. Rep. *7*, 10241 (2017). https://doi.org/10.1038/s41598-017-10662-x

[27] Y. Qi, T. Cagin, W.L. Johnson, W.A. Goddard III. J. Chem. Phys. **115**, 385 (2001). https://doi.org/10.1063/1.1373664

[28] A. Safaei, M. Attarian Shandiz, S. Sanjabi, Z.H. Barber. J. Phys. Chem. C **112**, 99 (2008).
https://doi.org/10.1021/jp0744681

[29] S. Xiong, W. Qi, Y. Cheng, B. Huang, M. Wang, Y. Li. Phys. Chem. Chem. Phys. **13**, *22*, 10652 (2011).
https://doi.org/10.1039/c0cp90161j

[30] V.M. Samsonov, S.A. Vasiliev, A.G. Bembel. PhMM **117**, *8*, 775 (2016). https://doi.org/10.7868/S0015323016080131

[31] K.K. Nanda. Phys. Lett. A **376**, *19*, 1647 (2012).
https://doi.org/10.1016/j.physleta.2012.03.055

[32] G. Guisbiers, M. Kazan, O. Van Overschelde, M. Wautelet, S. Pereira. J. Phys. Chem. C **112**, 4097 (2008).
https://doi.org/10.1021/jp077371n

[33] G.M. Poletaev, A.A. Sitnikov, V.I. Yakovlev, V.Yu. Filimonov. ZhETF **161**, *2*, 221 (2022). (in Russian).
https://doi.org/10.31857/S0044451022020079

[34] D. Prokoshkina, V.A. Esin, G. Wilde, S.V. Divinski. Acta Mater. **61**, *14*, 5188 (2013).
https://doi.org/10.1016/j.actamat.2013.05.010

[35] A.L. Petelin, A.A. Novikov, I.V. Apykhtina. Mater. Sci. Eng. **4**, *1*, 9 (2020). https://doi.org/10.15406/mseij.2020.04.00119

*Translated by A.Akhtyamov*